Hindawi
Wireless Communications and Mobile Computing
Volume 2018, Article ID 1802063, 9 pages
https://doi.org/10.1155/2018/1802063

Research Article

Dynamic Power Splitting Strategy for SWIPT Based Two-Way Multiplicative AF Relay Networks with Nonlinear Energy Harvesting Model

Tianci Wang,[1] **Guangyue Lu**,[1] **Yinghui Ye**,[1,2] **and Yuan Ren**[1]

[1]*Shaanxi Key Laboratory of Information Communication Network and Security, Xi'an University of Posts and Telecommunications, Xi'an, China*
[2]*Integrated Service Networks Lab of Xidian University, Xi'an, China*

Correspondence should be addressed to Yinghui Ye; connectyyh@126.com

Received 8 March 2018; Accepted 7 May 2018; Published 11 June 2018

Academic Editor: Wolfgang H. Gerstacker

This paper investigates an energy-constrained two-way multiplicative amplify-and-forward (AF) relay network, where a practical nonlinear energy harvesting (NLEH) model is equipped at the relay to realize simultaneous wireless information and power transfer (SWIPT). We focus on the design of dynamic power splitting (DPS) strategy, in which the PS ratio is able to adjust itself according to the instantaneous channel state information (CSI). Specifically, we first formulate an optimization problem to maximize the outage throughput, subject to the NLEH. Since this formulated problem is nonconvex and difficult to solve, we further transfer it into an equivalent problem and develop a Dinkelbach iterative method to obtain the corresponding solution. Numerical results are given to verify the quick convergence of the proposed iterative method and show the superior outage throughput of the designed DPS strategy by comparing with two peer strategies designed for the linear energy harvesting (LEH) model.

1. Introduction

Internet of things (IoT) devices are usually powered by batteries with limited energy storage capacity, leading to a key constraint of the performance of energy-constrained wireless networks [1, 2]. To address this problem, simultaneous wireless information and power transfer (SWIPT) has been recently proposed as a promising solution to prolong the lifetime of energy-constrained wireless networks, where the wireless signal is either switched in the time domain or split in the power domain to provide signal transmission and power transfer using the same wireless carrier, i.e., time switching (TS) strategy and power splitting (PS) strategy. Accordingly, SWIPT is applicable in energy-constrained networks for striking a balance between information and energy [3–5].

Relaying techniques, including one-way relay networks (OWRNs) and two-way relay networks (TWRNs), are highly beneficial in wireless communications to overcome shadowing effects, to increase the communication range, to improve the energy efficiency, and to increase the achievable throughput [6]. Of particular interest is the two-step (or three-step) TWRNs, in which one node shares its data with the other node via an intermediate relay. The system configuration may arise in many practical scenarios, e.g., data exchange between sensor nodes and the data through an immediate relay in IoT networks [7, 8]. However, in fact, the relay nodes may have limited battery capacity and thus rely on some external resources to charge in order to remain active. Further, due to the random positions of relay nodes, consistent power supply may be unavailable for energy-constrained relay nodes, leading to possible power outages. As a result, the aforementioned two promising techniques, SWIPT and two-step (or three-step) TWRNs, can be integrated to balance between information and energy [9].

Up to now, several works have been reported regarding this issue [10–15]. Authors of [10, 11] introduced decode-and-forward (DF) and amplify-and-forward (AF) into PS strategy based SWIPT with two-step TWRNs, respectively. Reference

[12] studied the optimal PS strategy to maximize the energy efficiency. Since the circuitry design of three-step is simpler than that of two-step, [13] studied the bounds performance for PS based SWIPT with three-step DF-TWRNs in terms of outage probability. Different from [13], the authors of [14] studied the PS based three-step multiplicative AF-TWRNs, due to the advantage of three-step multiplicative TWRNs in outage probability and investigated the corresponding outage performance with a static PS strategy, where the PS ratio is determined by statistic channel state information (CSI). This results in a room for improving by making full use of the instantaneous CSI. Due to this reason, the dynamic PS (DPS) strategy was further developed [15]. It was shown that the outage performance can be improved by employing the DPS strategy.

However, the above works discussed [10–15] were based on the assumption of a linear energy harvesting (LEH) model, which was shown to be inaccurate and not capable of capturing the nonlinear behaviour of RF energy harvesting (RF-EH) circuits [16]. As a result, those existing strategies based on the LEH model lead to significant performance loss in a real scenario owing to the mismatching between linear and nonlinear EH (NLEH) model. Even though several works [16–27] have been reported regarding the applications of the NLEH model for wireless communications, most of them (see [16–24]) focused on the wireless powered communication (WPC) networks and point-to-point/cognitive radio networks with SWIPT. Apart from the aforementioned networks, the applications of a NLEH model have also been studied to the OWRNs [25–27]. In [25, 26], the authors investigated the outage performance of a NLEH relaying network with a PS strategy. Considering the perfect/imperfect CSI at the relay, the optimal PS strategy was developed in terms of outage performance [27]. However, there is no work in the existing literature studying the TWRNs with a NLEH harvester. This motivates our work.

In this paper, we study a DPS strategy for three-step multiplicative AF-TWRNs, where the relay is equipped with a NLEH harvester (this work extends the recent work [15] into the NLEH) to realize the SWIPT. To incentivize the relay to cooperate with the source, the harvest-then-forward scheme is adopted, i.e., the relay only uses the harvested energy from the source's signal to assist its transmissions. In order to investigate the upper bound outage throughput of the considered network, we assume that CSI is available. Our contributions are as follows.

We formulate an optimization problem to maximize the outage throughput by adjusting the PS ratio according to the instantaneous CSI. The optimization problem is equivalent to maximize worse end-to-end signal-to-noise ratio (SNR), which is nonconvex and difficult to solve. On this basis, we reformulate it as a fractional programming problem and employ the Dinkelbach method to derive a DPS strategy. The simulation results show, compared with the existing strategies, the proposed DPS strategy achieves a larger outage throughput.

The rest of this paper is organized as follows. In Section 2, we introduce the system model. In Section 3, we formulate an optimization problem to maximize outage throughput and design an iterative method to obtain the optimal solution. Section 4 provides simulation results to verify our work. Finally, Section 5 concludes the paper.

2. System Model

2.1. Multiplicative AF-TWRNs. We consider a NLEH multiplicative AF-TWRNs, where an energy-constrained relay R coordinates the two-way communications for two terminals (i.e., node 1 and node 2) exchanging information by adopting the harvest-then-forward scheme, as shown in Figure 1. All nodes are equipped with one antenna due to the limited space (since the main focus of this work is on the novel dynamic power splitting (DPS) scheme design subject to the nonlinear model, for analytical tractability, we consider the single antenna AF relay networks). We ignore the direct transmission between two terminals due to the heavy fading [15]. For successful information exchange between the two nodes, we consider the following assumptions [14, 15]:

(i) The total transmission time block $T = 1$ is divided into three consecutive equal time slots, as shown in Figure 2. First, node 1 sends the signal to R. And then, node 2 sends the signal to R. Finally, the relay R broadcasts the multiplied signal to nodes k ($k = 1$ or 2) using the harvested energy.

(ii) The path-loss model is distance-dependent with a rate of $d_k^{-\alpha}$, where α is the path-loss exponent and d_k is the distance between node k and relay R. Let g_k denote the complex channel coefficients from the relay to the destination node k, respectively. Each link is independent with frequency nonselective Rayleigh block fading. Further, CSI is available in order to investigate the upper bound outage performance.

(iii) The processing energy required by the transmit/receive circuitry at the relay is ignored since it is very small compared with the transmit energy.

2.2. Energy Harvesting Model. EH model is able to characterize the relationship between input power P_{in} and output power P_{out} by a function $f(\cdot)$, given by

$$P_{out} = f\left(P_{in}\right). \tag{1}$$

The conventional LEH model assumes a fixed constant to describe the relationship between input power P_{in} and output power P_{out}, given by

$$P_{out}^{linear} = f\left(P_{in}\right) = \eta P_{ER_k}, \quad 0 \leqslant \eta \leqslant 1, \tag{2}$$

where η is the fixed energy conversion efficiency of energy harvester equipped at relay.

However, the above LEH model cannot capture the properties of practical EH circuits, since the energy conversion efficiency improves as the input power rises, but for high input power there is a limitation on the maximum harvested

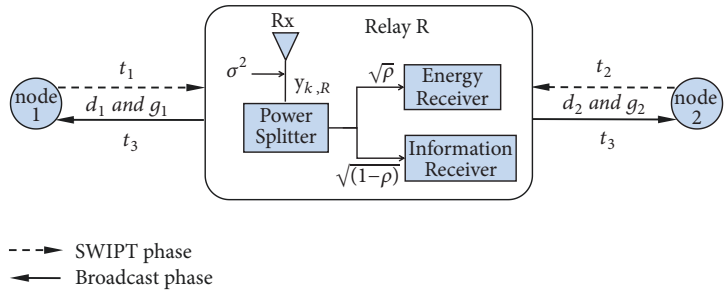

Figure 1: System model of three-step multiplicative AF-TWRNs with SWIPT.

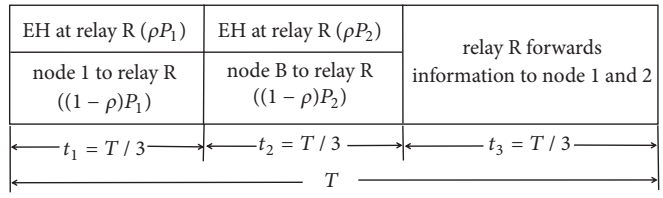

Figure 2: Transmission time-block structure for the DPS strategy.

energy [19]. To this end, a NLEH model was proposed by fitting the measurement data in [16], given by

$$P_{out}^{Non-linear} = f\left(P_{in}\right) = \frac{\left[M/\left(1+\exp\left(-\overline{a}\left(P_{in}-\overline{b}\right)\right)\right)-M\Omega\right]}{1-\Omega}, \quad (3)$$

where M denotes the maximum harvested power at EH harvester when the EH circuit is saturated; $\overline{a}$ and $\overline{b}$ are constants related to the detailed EH circuit specifications such as the resistance, capacitance, and diode turn-on voltage; $\Omega = 1/(1+\exp(\overline{a}\overline{b}))$.

More recently, the authors of [28] proposed another function to characterize the practical EH circuitry; that is,

$$P_{out}^{Non-linear} = f\left(P_{in}\right) = \frac{aP_{in}+b}{P_{in}+c} - \frac{b}{c}, \quad (4)$$

where parameters a, b, and c are constants determined by standard curve fitting tool.

Compared with the model in (3), the model in (4) is more mathematically tractable and is able to provide sufficient precision [28]. For the above reasons, this paper employs the model in (4) to develop the DPS strategy.

2.3. Working Flow. In the first or second slot, the signal from the node k received at relay R is given as

$$y_{k,R} = \sqrt{P_k}h_k x_k + z_k, \quad \forall k = 1, 2. \quad (5)$$

where P_k is the transmit power of node k, $h_k = g_k/\sqrt{d_k^{\alpha}}$, x_k denotes the normalized signal from the node k, and z_k is the additive white Gaussian noise (AWGN) at the receiving antenna.

The received RF signal is split into two streams, $\sqrt{(1-\rho)}y_{k,R}$ for information processing and $\sqrt{\rho}y_{k,R}$ for EH. Accordingly, based on model (4), the total harvested energy at R from the first and second slots can be calculated as

$$\begin{aligned} E_R &= \frac{T}{3}\left(P_{ER_1}^{Non-linear} + P_{ER_2}^{Non-linear}\right) \\ &= \frac{T}{3}\left(\frac{aP_{ER_1}+b}{P_{ER_1}+c} + \frac{aP_{ER_2}+b}{P_{ER_2}+c} - \frac{2b}{c}\right) \\ &= \frac{T}{3}\left(\frac{(ac-b)\left[2P_{ER_1}P_{ER_2} + c\left(P_{ER_1}+P_{ER_2}\right)\right]}{cP_{ER_1}P_{ER_2} + c^2\left(P_{ER_1}+P_{ER_2}\right)+c^3}\right), \end{aligned} \quad (6)$$

where $P_{ER_k} = \rho P_k |h_k|^2$ is the received power from the node k; $\rho \in [0, 1)$ is the PS ratio.

In the third slot, the received signals at the first slot and the second slot are multiplied and amplified, resulting in a hybrid signal at relay R, given by

$$\begin{aligned} y_R = \sqrt{\frac{P_R}{\xi}}&\left(h_1\sqrt{(1-\rho)P_1}x_1 + Z_1\right) \\ &\cdot\left(h_2\sqrt{(1-\rho)P_2}x_2 + Z_2\right), \end{aligned} \quad (7)$$

where $\xi = \Pi_{k=1}^{2}((1-\rho)|h_k|^2 P_k + \sigma_k^2)$ is the power constraint factor; σ_k^2 is the power of the mixed AWGN noises Z_k, including the antenna noise and conversion noise; $P_R = 3E_R/T$ is the transmitted power at the relay.

According to the single channel separation signal technology [15], the desired signal from the target node can be obtained from the mixed signal. Therefore, the signal received at destination node 1 obtains the information from node 2; that is,

$$y_{1,2} = x_1^{-1}\left(h_1 y_R + \widehat{Z}_1\right), \quad (8)$$

where $\widehat{Z}_1$ denotes the mixed noise at node 1 with the variance $\widehat{\sigma}_1^2$, which includes the transmitter antenna noise, the receiver antenna noise, and the conversion noise; $x_1^{-1} = 1/x_1$.

Substituting (7) into (8), the received signal $y_{1,2}$ at the node 1 from the node 2 can be rewritten as

$$y_{1,2} = \underbrace{\sqrt{\frac{P_R P_1 P_2}{\xi}}(1-\rho)|h_1|^2 h_2 x_2}_{\text{Signal Term}} + \underbrace{\sqrt{\frac{P_R}{\xi}}h_1 x_1^{-1} Z_1 Z_2 + \sqrt{\frac{P_R P_1 (1-\rho)}{\xi}}|h_1|^2 Z_2}_{\text{Noise Term I}} + \underbrace{\sqrt{\frac{P_R P_2 (1-\rho)}{\xi}}h_1 h_2 x_1^{-1} x_2 Z_1 + x_1^{-1}\widehat{Z}_1}_{\text{Noise Term II}}, \quad (9)$$

Therefore, the SNR from node 2 to node 1 can be described as

$$\gamma_1 = \frac{s}{n+o+i+e}, \quad (10)$$

where (in this paper, we assume that instantaneous CSI is only available at the relay in order to reduce the CSI feedback overhead. Thus, we assume that $P_1 = P_2 = P_S$, and the power allocation scheme for destination nodes has not been considered)

$$\begin{aligned}
s &= \mu\left[2P_{ER_1}P_{ER_2} + c\left(P_{ER_1} + P_{ER_2}\right)\right]P_S{}^2(1-\rho)^2|h_1|^4 \cdot |h_2|^2,\\
n &= \mu\left[2P_{ER_1}P_{ER_2} + c\left(P_{ER_1} + P_{ER_2}\right)\right]P_S(1-\rho)|h_1|^4\sigma_2^2,\\
o &= \mu\left[2P_{ER_1}P_{ER_2} + c\left(P_{ER_1} + P_{ER_2}\right)\right]P_S(1-\rho)|h_1|^2 \cdot |h_2|^2\sigma_1^2,\\
i &= \mu\left[2P_{ER_1}P_{ER_2} + c\left(P_{ER_1} + P_{ER_2}\right)\right]|h_1|^2\sigma_1^2\sigma_2^2,\\
e &= \left(cP_{ER_1}P_{ER_2} + c^2\left(P_{ER_1} + P_{ER_2}\right) + c^3\right) \cdot \left(P_S(1-\rho)|h_1|^2 + \sigma_1^2\right)\left(P_S(1-\rho)|h_2|^2 + \sigma_2^2\right)\widehat{\sigma}_1^2,\\
\mu &= ac - b,\\
P_1 &= P_2 = P_S,\\
P_{ER_1} &= \rho P_S|h_1|^2,\\
P_{ER_2} &= \rho P_S|h_2|^2.
\end{aligned} \quad (11)$$

Likewise, the SNR from the node 1 to node 2 is γ_2, which can be written as

$$\gamma_2 = \frac{s'}{n'+o'+i'+e'}, \quad (12)$$

where

$$\begin{aligned}
s' &= \mu\left[2P_{ER_1}P_{ER_2} + c\left(P_{ER_1} + P_{ER_2}\right)\right]P_S{}^2(1-\rho)^2|h_2|^4 \cdot |h_1|^2,\\
n' &= \mu\left[2P_{ER_1}P_{ER_2} + c\left(P_{ER_1} + P_{ER_2}\right)\right]P_S(1-\rho)|h_2|^4 \cdot \sigma_1^2,\\
o' &= \mu\left[2P_{ER_1}P_{ER_2} + c\left(P_{ER_1} + P_{ER_2}\right)\right]P_S(1-\rho)|h_2|^2 \cdot |h_1|^2\sigma_2^2,\\
i' &= \mu\left[2P_{ER_1}P_{ER_2} + c\left(P_{ER_1} + P_{ER_2}\right)\right]|h_2|^2\sigma_2^2\sigma_1^2,\\
e' &= \left(cP_{ER_1}P_{ER_2} + c^2\left(P_{ER_1} + P_{ER_2}\right) + c^3\right) \cdot \left(P_S(1-\rho)|h_2|^2 + \sigma_2^2\right)\left(P_S(1-\rho)|h_1|^2 + \sigma_1^2\right)\widehat{\sigma}_2^2.
\end{aligned} \quad (13)$$

3. Dynamic Power Splitting

3.1. Optimization Problem Formulated. For SWIPT based TWRNs, the outage occurs if one destination node cannot decode the information from the other source node. Thus, the outage throughput τ can be described as

$$\tau = (1 - P_{out})U, \quad (14)$$

with

$$\begin{aligned}
P_{out} &= P\{(\gamma_1 < \gamma_{th}) \cup (\gamma_2 < \gamma_{th})\}\\
&= 1 - P\{\gamma_1 \geqslant \gamma_{th}, \gamma_2 \geqslant \gamma_{th}\},
\end{aligned} \quad (15)$$

where $\gamma_{th} = 2^U - 1$ is the minimum acceptable threshold value; U denotes the constant transmission rate of the source node.

It can be observed from (14) and (15) that the outage throughput is determined by the worse end-to-end SNR of the two links. Thus, the optimization problem to maximize the outage throughput can be written as

$$\begin{aligned}
(\text{P1}): \quad &\max_{\rho} \min\{\gamma_1, \gamma_2\}\\
\text{subject to}: \quad &0 \leqslant \rho < 1.
\end{aligned} \quad (16)$$

Lemma 1. P1 *is proved to be equivalent to the following optimization problem* P2*, which is*

$$\begin{aligned}
(\text{P2}): \quad &\max_{\rho} \gamma\\
\textit{subject to}: \quad &0 \leqslant \rho < 1,
\end{aligned} \quad (17)$$

where $\gamma = \begin{cases} \gamma_1, & \text{if } \gamma_1 \leqslant \gamma_2 \\ \gamma_2, & \text{if } \gamma_1 > \gamma_2 \end{cases}$.

The proof is given in Appendix.

3.2. Iterative Method Design. In this subsection, we focus on the design of iterative method to solve (P2) based on the **Lemma 1**. Specifically, we assume that γ_1 is equal to γ and design an iterative method to obtain corresponding solution. Note that the case of $\gamma = \gamma_2$ can also be obtained by the same method.

We denote the maximum SNR of the node 2 to node 1 which equals q^*, which is

$$q^* = \max_{0 \leqslant \rho^{(l)} < 1} \frac{s}{n + o + i + e}, \tag{18}$$

It can be concluded that (18) is a typical fractional programming problem. Therefore, we can employ the Dinkelbach method to obtain the maximum q^*, as shown in Algorithm 1. Notice that q^* is available if and only if

$$\max_{0 \leqslant \rho^{(l)} < 1} \left\{ s - q^* \left(n + i + s + e \right) \right\} = 0. \tag{19}$$

The proof can be found in [29].

Next, we solve the auxiliary problem in the step 4 of the Dinkelbach method, which is nonconvex. The equation in the auxiliary problem can be written as

$$F\left(q^{(l-1)}, \rho^{(l)}\right) = r_1 \rho^4 + r_2 \rho^3 + r_3 \rho^2 + r_4 \rho - r_5, \tag{20}$$

where

$$\begin{aligned}
r_1 &= 2\mu m_1 m_3 - u_5 m_1^2, \\
r_2 &= \mu \left[-4 m_1 m_3 + \left(c + 2u_4 \right) m_2 m_3 \right] \\
&\quad - u_5 \left(u_8 m_1 m_2 - 2 m_1^2 \right), \\
r_3 &= \mu \left[2 \left(m_3 - m_8 \right) m_1 + c m_2 m_7 - 2 c m_3 \right], \\
&\quad - k_5 \left[\left(u_9 + u_{10} m_2 \right) m_1 + m_1^2 - u_3 m_2^2 \right], \\
r_4 &= \mu \left(c m_3 - c m_8 \right) \\
&\quad - u_6 \left[\left(m_2 - 2c \right) m_1 - u_3 m_2 + u_{11} m_2^2 \right], \\
r_5 &= u_7 \left(m_1 + \sigma^2 m_2 + \sigma^4 \right).
\end{aligned}$$

$$\begin{aligned}
m_1 &= u_1 u_2, \\
m_2 &= u_1 + u_2, \\
m_3 &= u_1 u_2 \left| h_1 \right|^2, \\
m_4 &= u_1 u_4 \left| h_1 \right|^2, \\
m_5 &= u_2 u_4 \left| h_1 \right|^2, \\
m_6 &= u_4 \left| h_1 \right|^2 \sigma_1^2, \\
m_7 &= u_4 \left| h_1 \right|^2 \left(u_1 + u_2 \right), \\
m_8 &= k_4 \left| h_1 \right|^2 \left(u_1 + u_2 + \sigma^2 \right).
\end{aligned}$$

$$\begin{aligned}
u_1 &= P_S \left| h_1 \right|^2, \\
u_2 &= P_S \left| h_2 \right|^2, \\
u_3 &= c\sigma^2, \\
u_4 &= q^{(l-1)} \sigma^2, \\
u_5 &= q^{(l-1)} \sigma^2 c, \\
u_6 &= q^{(l-1)} \sigma^2 c^2, \\
u_7 &= q^{(l-1)} \sigma^2 c^3, \\
u_8 &= c - \sigma^2, \\
u_9 &= \sigma^4 + c^2, \\
u_{10} &= \sigma^2 - 2c, \\
u_{11} &= \sigma^2 + \sigma^4.
\end{aligned} \tag{21}$$

The first-order derivative of the function $F(q^{(l-1)}, \rho^{(l)})$ can be written as

$$F'\left(q^{(l-1)}, \rho^{(l)}\right) = 4 r_1 \rho^3 + 3 r_2 \rho^2 + 2 r_3 \rho + r_4 = 0. \tag{22}$$

Clearly, (22) is a typical cubit equation and the roots can be determined [30]. For the convenience of the following description, we denote that $A = 9r_2^2 - 24 r_1 r_3$, $B = 6 r_2 r_3 - 36 r_1 r_4$, $C = 4 r_3^2 - 9 r_2 r_4$, and $\Delta = B^2 - 4AC$. The roots are as follows.

Case 1. If $A = B = 0$, there exists a triple root and the real root is $-3r_2/12r_1$.

Case 2. If $\Delta = B^2 - 4AC > 0$, there exist one real root and two complex roots. The real root is $(-3r_2 - (\sqrt[3]{Y_1} + \sqrt[3]{Y_2}))/12r_1$, where $Y_{1,2} = 3Ar_2 + 12r_1((-B \pm (\sqrt{B^2 - 4AC}))/2)$.

Case 3. If $\Delta = B^2 - 4AC = 0$, there exist a double real root, and a real root, i.e., two different real roots. Both two different roots are $-K/2$ and $-3r_2/4r_1 + K$, where $K = (B/A)(A \neq 0)$.

Case 4. If $\Delta = B^2 - 4AC < 0$, there exist three different real roots. Three different real roots are $(-3r_2 - 2\sqrt{A}\cos(\theta/3))/12r_1$, $(-3r_2 + \sqrt{A}(\cos(\theta/3) + \sqrt{3}\sin(\theta/3)))/12r_1$, and $(-3r_2 + \sqrt{A}(\cos(\theta/3) - \sqrt{3}\sin(\theta/3)))/12r_1$, where $\theta = \arccos T$ and $T = (6Ar_2 - 12r_1 B)/2\sqrt{A^3} (A > 0, -1 < T < 1)$.

Based on the above cases, we can obtain closed-form roots for the above cubic equation (22). Then the real root from 0 to 1 to maximize the function $F(q^{(l-1)}, \rho^{(l)})$ is selected as the optimal solution to the auxiliary problem by comparing values of the real roots.

4. Simulation Results

In this section, we present the numerical results to evaluate the outage throughput of the proposed DPS, two baseline schemes proposed in [14, 15] under a NLEH model. The fitted ones of the employed NLEH parameters are set as $a = 109.7$,

(1): Initialize:
the maximum number of iterations $L_{\max}$, the iteration index $l = 1$, $q^{(0)} = 0$;
(2): Set:
η, P_S, δ, σ^2 and input the instantaneous CSI, h_k;
(3): **repeat**
(4): Solve the maximize optimization problem in (19) with $F(q^{(l-1)}, \rho^{(l)}) = \max_{0 \leqslant \rho^{(l)} < 1}\{s - q^{(l-1)}(n + o + i + e)\}$ and obtain $\widetilde{\rho}^{(l)}$;
(5): Apply $\widetilde{\rho}^{(l)}$ into s, n, o, i, e to calculate $\widetilde{s}$, $\widetilde{n}$, $\widetilde{o}$, $\widetilde{i}$, $\widetilde{e}$;
(6): Update $q^{(l)} = \widetilde{s}/(\widetilde{n} + \widetilde{o} + \widetilde{i} + \widetilde{e})$;
(7): If $|F(q^{(l-1)}, \widetilde{\rho}^{(l)})| \geqslant \delta$, then $l = l + 1$;
(8): **until** $|F(q^{(l-1)}, \widetilde{\rho}^{(l)})| < \delta$ or $l = L_{\max}$;
(9): Obtain the maximum SNR $q^* = q^{(l)}$, and the optimal PS ratio $\rho^* = \widetilde{\rho}^{(l)}$.

Algorithm 1: The proposed iterative method.

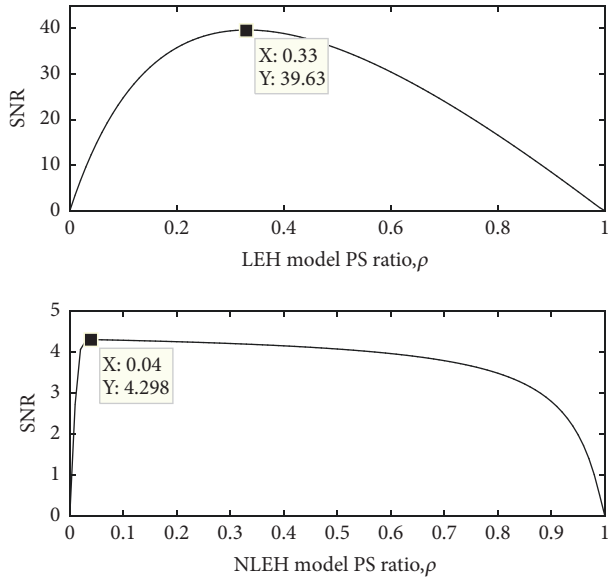

Figure 3: SNR versus PS ratio through exhaustive searching.

b = 43.69, and c = 128.1. For comparison, we set the parameters as follows: $\alpha = 2.7$, $d_1 = d_2 = 1$m, $\delta = 10^{-1}$, and $\sigma^2 = 0.01$.

Figure 3 shows the SNR versus PS ratio by exhaustive searching method with the channel gains $|h_1| = 0.9770$ and $|h_2| = 1.2594$. The transmit power and the transmission rate of source node are set to be 1.5 J/s and 3 bits/s/Hz, respectively. One can see that the value of optimal PS ratios for LEH and NLEH is unequal. This point illustrates that the optimal PS strategy designed for LEH is not an optimal one for NLEH, due to the mismatching between LEH and NLEH. Based on the same parameter as Figure 3, the PS ratio and SNR versus number of iterations are illustrated. It can be observed that only two iterations are required to obtain optimal solution by the proposed iterative method. In addition, the optimal solution obtained by the proposed iterative method is equal to the one obtained by exhaustive searching method in Figure 4. The above analyses verify our proposed iterative method.

Figure 5 depicts the outage throughput with different transmission rates U for the proposed DPS strategy, the static PS strategy [14], and the existing DPS strategy (here, we employ LEH-DPS scheme to calculate the optimal PS ratio under the LEH model and substitute it into NLEH model) [15]. Among those strategies, the static PS strategy and the existing DPS strategy are designed for LEH model and the existing DPS strategy is renamed as a baseline scheme for convenience. It can be observed that, in terms of outage throughput, the proposed DPS scheme outperforms the static PS and the baseline scheme at different transmission rates U, as expected. This is because our proposed strategy is designed for NLEH and can obtain the optimal solution optimized for a NLEH model.

Both Figures 6 and 7 illustrate the outage throughput versus SNR for two strategies under different scenarios. One can see from Figure 6 that the outage throughput decreases with the distance. The reason is that the larger distance leads to a smaller channel gain and a lower outage throughput. One also can see that the proposed strategy outperforms the baseline scheme, which shows that the baseline scheme is a suboptimal one for the NLEH. In addition, it can be observed from Figure 7 that a considerable performance gain can be achieved by selecting an appropriate transmission rate.

5. Conclusion

In this paper, we developed a DPS strategy to maximize the outage throughput for NLEH three-step multiplicative AF-TWRNs. In particular, we formulated a nonconvex optimization problem for maximizing the outage throughput and proposed a Dinkelbach method to obtain the solution with a few iterations. Although the auxiliary problem of the proposed Dinkelbach method is nonconvex, we derived the closed-form solutions and avoided the necessity of solving a sequence of nonconvex auxiliary problems. Simulations showed that the proposed DPS strategy achieves a higher outage throughput in NLEH three-step multiplicative AF-TWRNs compared with two recent schemes designed for the LEH model.

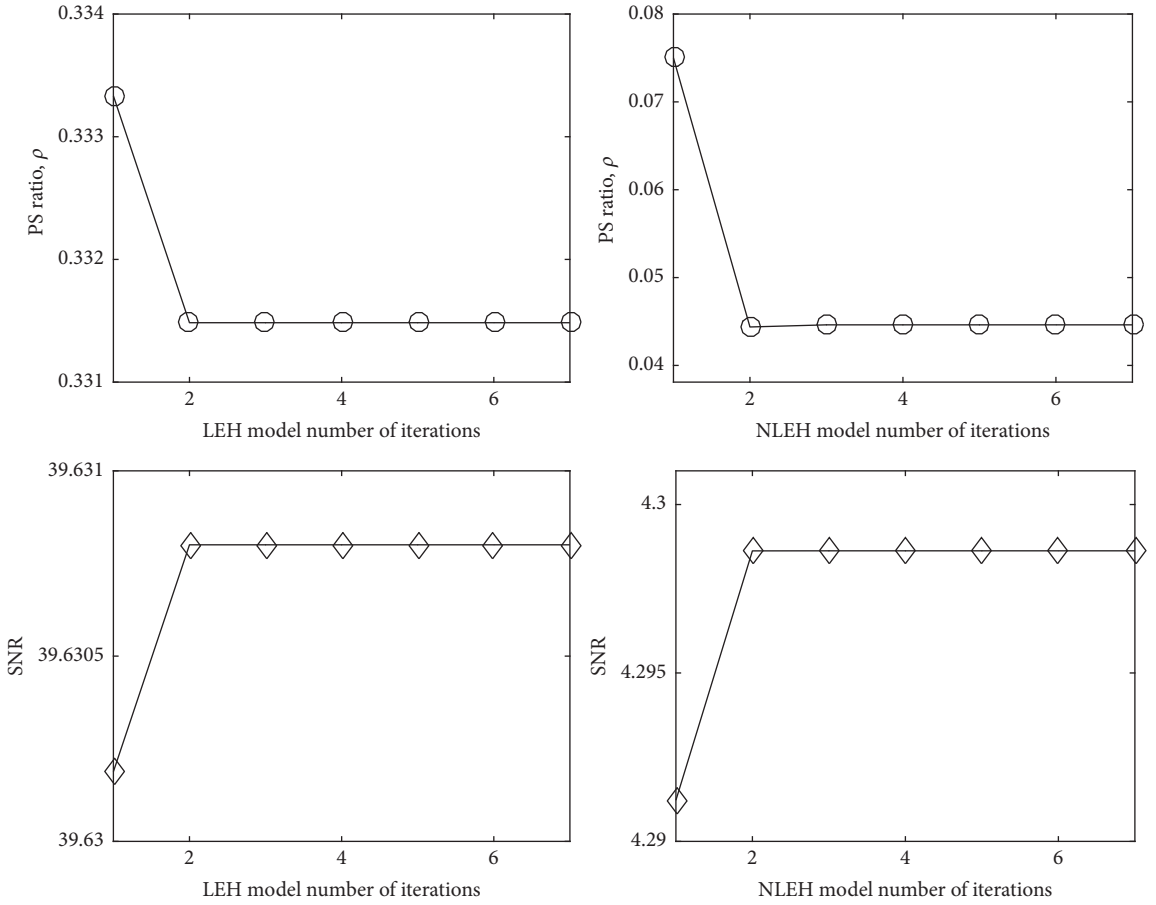

FIGURE 4: PS ratio and SNR versus number of iterations.

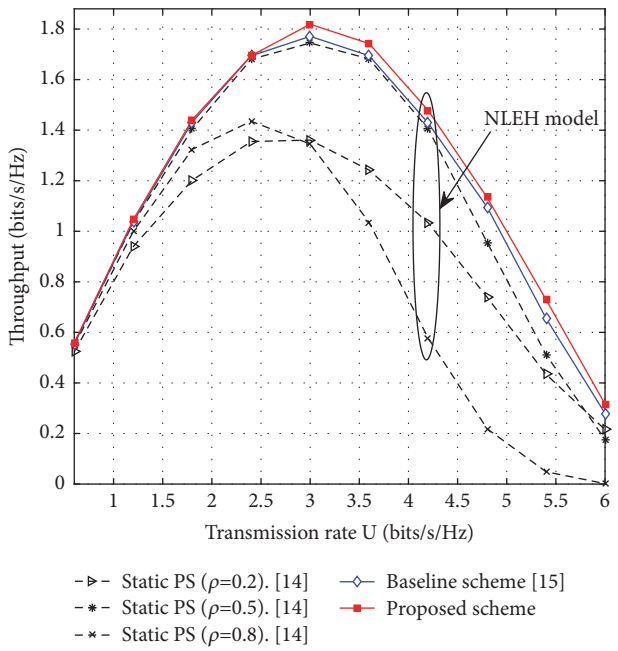

FIGURE 5: Outage throughput versus varying values of transmission rate.

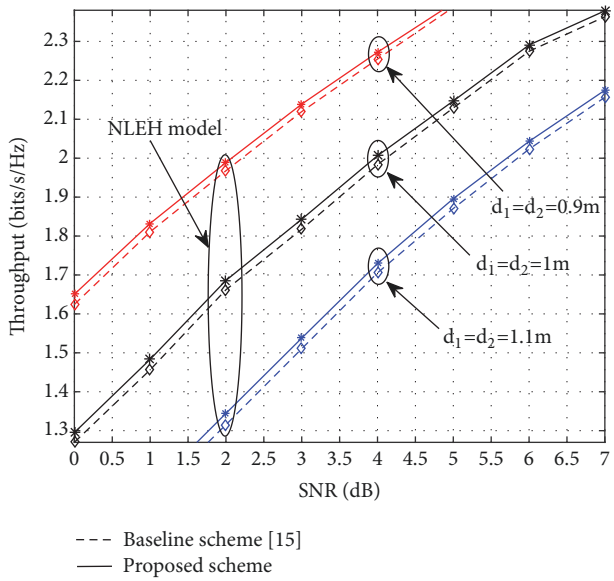

Figure 6: Outage throughput versus SNR with different distances.

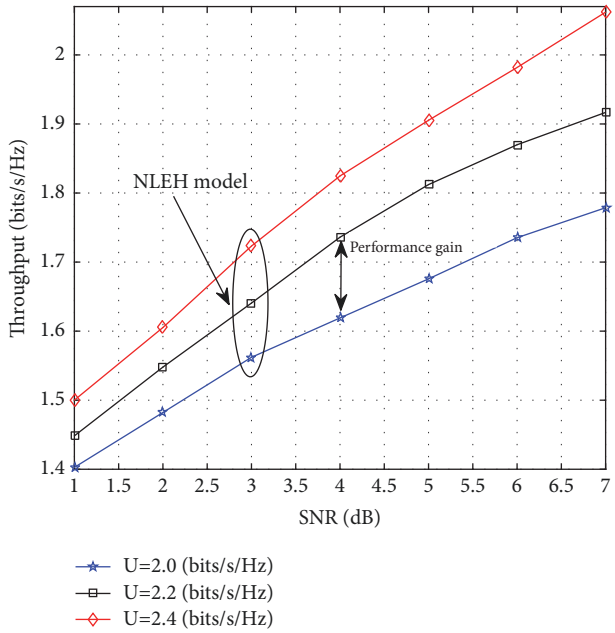

Figure 7: Outage throughput versus SNR with different transmission rates.

Appendix

Proof of the Lemma

For ease of analysis, we neglect the antenna noise and assume that $\sigma^2 = \sigma_1^2 = \sigma_2^2 = \widetilde{\sigma}_1^2 = \widetilde{\sigma}_2^2$ [14, 15].

Case i. If $|h_1|^2 = |h_2|^2$ or $\rho = 0$, it is obvious that $\gamma_1 = \gamma_2$. Thus, the optimization problem (P1) is equivalent to (P2).

Case ii. By means of reduction to absurdity, it can be proven that $\gamma_1 = \gamma_2$ holds when $|h_1|^2 \neq |h_2|^2$ and $\rho \neq 0$. We assume that $\gamma_1 - \gamma_2 = 0$ holds. Through some convenient mathematical calculations, the equality $\gamma_1 - \gamma_2 = 0$ can be rewritten as

$$\begin{aligned} &|h_1|^2 \left((1-\rho) P_S |h_1|^2 + \sigma^2\right) \left((1-\rho) P_S |h_2|^2 + \sigma^2\right) \\ &= |h_2|^2 \left((1-\rho) P_S |h_1|^2 + \sigma^2\right) \\ &\cdot \left((1-\rho) P_S |h_2|^2 + \sigma^2\right) \end{aligned} \tag{A.1}$$

Obviously, (A.1) holds if and only if $|h_1|^2 = |h_2|^2$ or $\rho = 0$, which indicates that the assumption $\gamma_1 - \gamma_2 = 0$ does not hold except for the case i. Based on the above cases, **Lemma 1** holds.

The proof is complete.

Data Availability

The data used to support the findings of this study are available from the corresponding author upon request.

Conflicts of Interest

The authors declare that they have no conflicts of interest.

Acknowledgments

The research reported in this article was supported by the National Science and Technology Major Project (2016ZX03001016), the Science and Technology Innovation Team of Shaanxi Province for Broadband Wireless and Application under Grant 2017KCT-30-02, the Natural Science Foundation of China (61701399, 61501371), and the Research Program of Education Bureau of Shaanxi Province (17JK0699).

References

[1] Z. Chu, F. Zhou, Z. Zhu, R. Q. Hu, and P. Xiao, "Wireless Powered Sensor Networks for Internet of Things: Maximum Throughput and Optimal Power Allocation," *IEEE Internet of Things Journal*, vol. 5, no. 1, pp. 310–321, Feb, 2018.

[2] F. Zhou, Y. Wu, Y. Liang, Z. Li, Y. Wang, and K. K. Wong, "State of the art, taxonomy, and open issues on NOMA in cognitive radio networks," *IEEE Wireless Communications Magazine*, vol. 25, no. 2, pp. 100–108, 2018.

[3] L. Shi, L. Zhao, K. Liang, and H. Chen, "Wireless Energy Transfer Enabled D2D in Underlaying Cellular Networks," *IEEE Transactions on Vehicular Technology*, vol. 67, no. 2, pp. 1845–1849, Feb, 2018.

[4] Y. Ye, Y. Li, D. Wang, and G. Lu, "Power splitting protocol design for the cooperative NOMA with SWIPT," in *Proceedings of the IEEE International Conference on Communications*, pp. 1–5, May 2017.

[5] D. Wang, Y. Li, Y. Ye, H. Xia, and H. Zhang, "Joint Time Allocation and Power Splitting Schemes for DF Energy Harvesting Relaying Networks," in *Proceedings of the IEEE 86th Vehicular Technology Conference*, pp. 1–5, September 2017.

[6] D. Gunduz, A. Yener, A. Goldsmith, and H. V. Poor, "The multiway relay channel," *IEEE Transactions on Information Theory*, vol. 59, no. 1, pp. 51–63, 2013.

[7] F. Zhou, Y. Wu, R. Q. Hu, Z. Li, and K. K. Wong, "Energy-efficient NOMA heterogeneous cloud radio access networks," *IEEE Wireless Communications Magazine*, 2017, to be published.

[8] B. Rankov and A. Wittneben, "Spectral efficient protocols for half-duplex fading relay channels," *IEEE Journal on Selected Areas in Communications*, vol. 25, no. 2, pp. 379–389, 2007.

[9] Z. Chu, M. Johnston, and S. Le Goff, "SWIPT for wireless cooperative networks," *IEEE Electronics Letters*, vol. 51, no. 6, pp. 536–538, 2015.

[10] S. Ghosh, T. Acharya, and S. P. Maity, "Outage analysis in DF relay assisted two-way communication with RF energy harvesting," in *Proceedings of the WSA 2017; 21th International ITG Workshop on Smart Antennas*, pp. 1–8, March, 2017.

[11] Z. Chen, B. Xia, and H. Liu, "Wireless information and power transfer in two-way amplify-and-forward relaying channels," in *Proceedings of the IEEE Global Conference on Signal and Information Processing*, pp. 168–172, December 2014.

[12] C. Zhang, H. Du, and J. Ge, "Energy-efficient power allocation in energy harvesting two-way AF relay systems," *IEEE Access*, vol. 5, pp. 3640–3645, 2017.

[13] N. T. P. Van, S. F. Hasan, X. Gui, S. Mukhopadhyay, and H. Tran, "Three-step two-way decode and forward relay with energy harvesting," *IEEE Communications Letters*, vol. 21, no. 4, pp. 857–860, 2017.

[14] S. T. Shah, K. W. Choi, S. F. Hasan, and M. Y. Chung, "Energy harvesting and information processing in two-way multiplicative relay networks," *IEEE Electronics Letters*, vol. 52, no. 9, pp. 751–753, 2016.

[15] Z. Wang, Y. Li, Y. Ye, and H. Zhang, "Dynamic Power Splitting for Three-Step Two-Way Multiplicative AF Relay Networks," in *Proceedings of the IEEE 86th Vehicular Technology Conference*, pp. 1–5, Sept, 2017.

[16] E. Boshkovska, D. W. K. Ng, N. Zlatanov, and R. Schober, "Practical non-linear energy harvesting model and resource allocation for SWIPT systems," *IEEE Communications Letters*, vol. 19, no. 12, pp. 2082–2085, Dec, 2015.

[17] D. Mishra, S. De, and D. Krishnaswamy, "Dilemma at RF Energy Harvesting Relay: Downlink Energy Relaying or Uplink Information Transfer?" *IEEE Transactions on Wireless Communications*, vol. 16, no. 8, pp. 4939–4955, Aug, 2017.

[18] E. Boshkovska, D. W. K. Ng, N. Zlatanov, A. Koelpin, and R. Schober, "Robust Resource Allocation for MIMO Wireless Powered Communication Networks Based on a Non-Linear EH Model," *IEEE Transactions on Communications*, vol. 65, no. 5, pp. 1984–1999, May, 2017.

[19] L. Shi, L. Zhao, K. Liang, X. Chu, G. Wu, and H. Chen, "Profit maximization in wireless powered communications with improved non-linear energy conversion and storage efficiencies," in *Proceedings of the IEEE International Conference on Communications*, pp. 1–6, May, 2017.

[20] K. Xiong, B. Wang, and K. J. R. Liu, "Rate-Energy Region of SWIPT for MIMO Broadcasting under Nonlinear Energy Harvesting Model," *IEEE Transactions on Wireless Communications*, vol. 16, no. 8, pp. 5147–5161, Aug, 2017.

[21] Q. Yao, T. Q. S. Quek, A. Huang, and H. Shan, "Joint Downlink and Uplink Energy Minimization in WET-Enabled Networks," *IEEE Transactions on Wireless Communications*, vol. 16, no. 10, pp. 6751–6765, Oct, 2017.

[22] Y. Wang, F. Zhou, Y. Wu, and H. Zhou, "Resource allocation in wireless powered cognitive radio networks based on a practical non-linear energy harvesting model," *IEEE Access*, vol. 5, pp. 17618–17626, 2017.

[23] J.-M. Kang, I.-M. Kim, and D. I. Kim, "Mode Switching for SWIPT over Fading Channel with Nonlinear Energy Harvesting," *IEEE Wireless Communications Letters*, vol. 6, no. 5, pp. 678–681, Oct, 2017.

[24] F. Zhou, Z. Chu, H. Sun, R. Q. Hu, and L. Hanzo, "Artificial Noise Aided Secure Cognitive Beamforming for Cooperative MISO-NOMA Using SWIPT," *IEEE Journal on Selected Areas in Communications*, 2018, to be published.

[25] A. Cvetkovic, V. Blagojevic et al., "Performance Analysis of Nonlinear Energy-Harvesting DF Relay System in Interference-Limited Nakagami-m Fading Environment," *ETRI Journal*, vol. 39, no. 6, pp. 803–812, Dec, 2017.

[26] J. Zhang and G. Pan, "Outage Analysis of Wireless-Powered Relaying MIMO Systems with Non-Linear Energy Harvesters and Imperfect CSI," *IEEE Access*, vol. 4, pp. 7046–7053, 2016.

[27] K. Wang, Y. Li, Y. Ye, and H. Zhang, "Dynamic Power Splitting Schemes for Non-Linear EH Relaying Networks: Perfect and Imperfect CSI," in *Proceedings of the IEEE 86th Vehicular Technology Conference*, pp. 1–5, Sept, 2017.

[28] Y. Chen, N. Zhao, and M. Alouini, "Wireless Energy Harvesting Using Signals From Multiple Fading Channels," *IEEE Transactions on Communications*, vol. 65, no. 11, pp. 5027–5039, 2017.

[29] W. Dinkelbach, "On nonlinear fractional programming," *Management Science*, vol. 13, no. 7, pp. 492–498, 1967.

[30] S. Fan, "A new extracting formula and a new distinguishing means on the one variable cubic equation," *Natural Science Journal of Hainan Teachers College*, vol. 2, no. 2, pp. 91–98, 1989.